ACI STRUCTURAL JOURNAL TECHNICAL PAPER

Title no. 100-S7

Seismic Behavior of Nonseismically Detailed Interior Beam-Wide Column Joints—Part II: Theoretical Comparisons and Analytical Studies

by Bing Li, Yiming Wu, and Tso-Chien Pan

The experimental results of four full-scale reinforced concrete interior beam-wide column joints with nonseismic detailing and limited seismic detailing have been presented in the previous paper. Due to the unique features of the test specimens and the inherent complexity of beam-column joints, however, such a study is not sufficient. Therefore, in this paper, an analytical investigation would be useful to provide a better understanding of the seismic behavior of such beam-wide column joints. The developed finite element models were described and verified using the results of the experimental results presented in the previous paper. The global behavior and the principal stresses of the interior beam-wide column joints were discussed and examined in detail. The calculated results indicated that global behavior of the joints can be simulated to correlate well with the experimental observations. In addition, the effects of several critical design parameters on the joint's behavior are explored by means of the developed finite element models; implications of the results on code specifications are discussed.

Keywords: ductility; joint; reinforced concrete.

INTRODUCTION

In Singapore, there are a large number of wide-column moment resisting frames built for residential and commercial purposes. The current Singapore building code is mainly based on the British Standard: the BS 8110,[1] which has no provision for seismic loading. Hence, almost all these frames are built without seismic consideration in design and detailing, for example, no joint reinforcement in the joint cores. Recent studies,[2] however, have shown that although Singapore is located in a low seismicity region and there has never been any earthquake damage in the country, the seismic hazard potential in the country should not be ignored. This makes it necessary to study the performance of these wide-column moment resisting frames under possible earthquake conditions, and as a critical part of such frames, the nonseismically detailed beam-wide column joints deserve more attention. In addition, beam-wide column joints have rarely been studied before, and this makes the study of such joints even more valuable and necessary.

Reliable information on the seismic behavior of full-scale beam-wide column joints can be obtained by experiments such as those reported and discussed in the previous paper. Experiments, however, are expensive and time consuming; thus, it is necessary to develop a numerical tool for the reasonable prediction of beam-wide column joints' behavior. To better understand the behavior of such joints, further discussions on these experimental results and comparison with theoretical results are presented in this paper. In this study, the nonlinear behavior of beam-wide column joints under reversed cyclic loading was analyzed by the finite element analysis method with the emphasis on the effect of joint transverse reinforcements, column axial load, and bond condition on the joint's behavior. By using this method, not only were the experimental results further verified and analyzed, but an investigation into the effects of some critical parameters has been carried out.

RESEARCH SIGNIFICANCE

The seismic behavior of beam-column joints is influenced by many parameters. Due to the inherent complexity of the joints, the effects of the combined effect of the parameters still have not been validated through many studies. In the experimental study, full-scale beam-wide column joints were tested; however, there was no column axial loading applied to the specimens. Column axial loading is one of the most controversial parameters and up until now, its effect has not been definitely decided. An analytical model that has been properly calibrated with available experimental results can be very useful for conducting parametric studies to enhance understanding. In this paper, the predictions of FEM models are compared with the experimental results, and parametric studies are conducted to quantify the major variables influencing the seismic behavior of beam-wide column joints.

ANALYTICAL MODELLING OF REINFORCED CONCRETE BEAM-WIDE COLUMN JOINTS

To supplement and further verify the test results obtained from the experimental work, the finite element method (FEM) was employed to improve the understanding of the structural response of the joints. The program used for the study was the FEM software package,[3] developed at the University of Tokyo. It includes nonlinear and path-dependent material constitutive models applicable to loading, unloading, and reloading as well. The software package[3] is capable of conducting a large-deformation nonlinear two-dimensional reinforced concrete structural system under static and dynamic loading using a multidirectional fixed smeared cracking feature. The finite element models of the joints are developed using the as-built dimensions and measured material properties to predict the local and global response of the test specimens and to provide better insight into the structural behavior of the joints.

ACI Structural Journal, V. 100, No. 1, January-February 2003.
MS No. 01-353 received October 26, 2001, and reviewed under Institute publication policies. Pertinent discussion will be published in the November-December 2003 *ACI Structural Journal* if received by July 1, 2003.

ACI member **Bing Li** *is an assistant professor in the School of Civil and Environmental Engineering at Nanyang Technological University, Singapore. He received his PhD from the University of Canterbury, New Zealand. His research interests include reinforced concrete and precast concrete structures, particularly in design for earthquake and blast resistance.*

ACI member **Yiming Wu** *is a research associate in the School of Civil and Environmental Engineering at Nanyang Technological University. He received his BEng from Tongji University, China, and his MEng from the Nanyang Technological University.*

Tso-Chien Pan *is a professor and Director of the Protective Technology Research Center in the School of Civil and Environmental Engineering at Nanyang Technological University. He received his PhD from the University of California at Berkeley, Calif. His research interests include damage assessment of buildings subjected to dynamic loading and vibration isolation for structures and equipment.*

Modeling of concrete

Concrete model prior to generation of cracks—In WCOMD-2D,[3] the model for concrete prior to cracking is constructed based on an elastic-plastic and fracture model.[4] The equivalent stress and equivalent strain relationship is formulated with the initial elastic modulus, the fracture parameter, and the equivalent plastic strain. In this model, the cracking criterion is determined mainly from the tensile stress and the effects of those factors, such as the size effect of the structural member, the method of curing, and shrinkage during drying, which are to be taken into account by modifying the uniaxial tensile strength. As for the fracture envelope under biaxial stress, the Aoyagi-Yamada model[5] was adopted. The uniaxial tensile strength of the concrete to be used is the value given from the cylinder compressive strength, which was reduced from 0.8 to 0.9 in consideration of the effects of the curing condition of the specimen[6]

$$f_t = 0.20 f_c'^{2/3} \tag{1}$$

Cracks do not appear as soon as the stress generated has attained its cracking level, but it takes the principal tensile strain to reach a limit strain. In this model, the tensile limit strain is twice as much as the tensile strain for the tensile strength of the concrete.[7] In case of reversed cyclic loading, cracks appear in different directions from those of existing cracks; the same criterion is applied as long as the angle of the cracks to existing cracks is greater than 15 degrees. If the angle is less than that, it is assumed that the secondary cracks will not be generated even when the tensile stress has reached the fracture envelope.[6]

Modeling of cracked concrete—

1. *Modeling of concrete under tensile stress*. Owing to the bonding of concrete to the reinforcing bars, the concrete continues to support a part of the tensile force even after cracking has taken place in a reinforced concrete. This maintains a higher level of the stiffness in the reinforced concrete than that of the reinforcing bars alone. To model this phenomenon, a tension stiffening model[6] was used

$$\sigma_t = f_t(\varepsilon_{tu}/\varepsilon_t)^c \tag{2}$$

where σ_t is the average tensile stress of concrete; f_t is the concrete's tensile strength; ε_{tu} is the tensile strain when the concrete tensile stress equals to f_t; ε_t is the concrete tensile strain; and $c = 0.4$ for deformed bars.

2. *Modeling of concrete under compressive stress*. The compressive stiffness of cracked concrete is lower than that in the uncracked state. Collins and Vecchio[8] developed an empirical formula for giving the reduction factor on their own experiments to decrease the stiffness of cracked concrete as a function of the tensile strain perpendicular to the crack plane. In this model, the same model for uncracked concrete is used by only modifying the fracture parameter as a function of the strain perpendicular to the crack plane.[8]

3. *Modeling of concrete under shear stress*. A simplified shear transfer model is used to model the concrete under shear stress by ignoring both the elastic component in the deformation at the crack plane and the effect of the crack width. The model gives the shear stress solely in terms of the ratio of shear displacement to crack width, regardless of the width of the crack[6]

$$\psi = \beta^2/(1+\beta^2) \tag{3}$$

where ψ is the ratio of shear stress to shear strength, and β is the ratio of shear displacement to crack width. In this formulation, the shear transfer stress is normalized by the shear transfer strength, which is expressed as a function of the cylinder compressive strength

$$f_{st} = 3.8 f_c'^{1/3} \tag{4}$$

Modeling of reinforcing bar in concrete

The constitutive model for the reinforcing bar in concrete has to be numerically modeled based both on the properties of the bars and on the effect of the bond to concrete. A numerical modeling of the bar on the basis of stress-strain envelope curves determined for typical domestically produced bars formulated by the steel strain at the onset of strain hardening and the subsequent form of the stress-strain curve from the yield point and the tensile strength[9] is adopted. For the unloading and reloading process, the Kato model[10] is used for its capability and for its ease in handling.

Bond-slip-strain model of deformed bar

For beam-column joints, the relative displacement between the steel bars and the surrounding concrete is recognized to be very large at the column and beam faces, where plastic hinges may form. The influence of bond slip on the behavior of the entire structure is considerably high. To formulate a bond-slip-strain relationship that holds good under any boundary conditions and any materials, in the FEM software package,[3] the bond stress is formulated as a function of strain multiplied by a function of slip, which is defined as the bond stress when the strain of the bar is zero[6]

$$\tau(\varepsilon, s) = \tau_o(s) g(\varepsilon) \tag{5}$$

where $\tau(\varepsilon,s)$ is a bond stress and $\tau_o(s)$ is a bond stress with zero strain.

ANALYSIS RESULTS AND COMPARISONS

Beam-wide column joint modeling

To analyze the joints, the finite element models have exactly the same geometry configuration and dimensions as the test specimens. The material properties of concrete and reinforcing steels were according to the measured values. For all specimens, the outermost meshes of the beams and columns were set so that the center of their meshes coincided with the

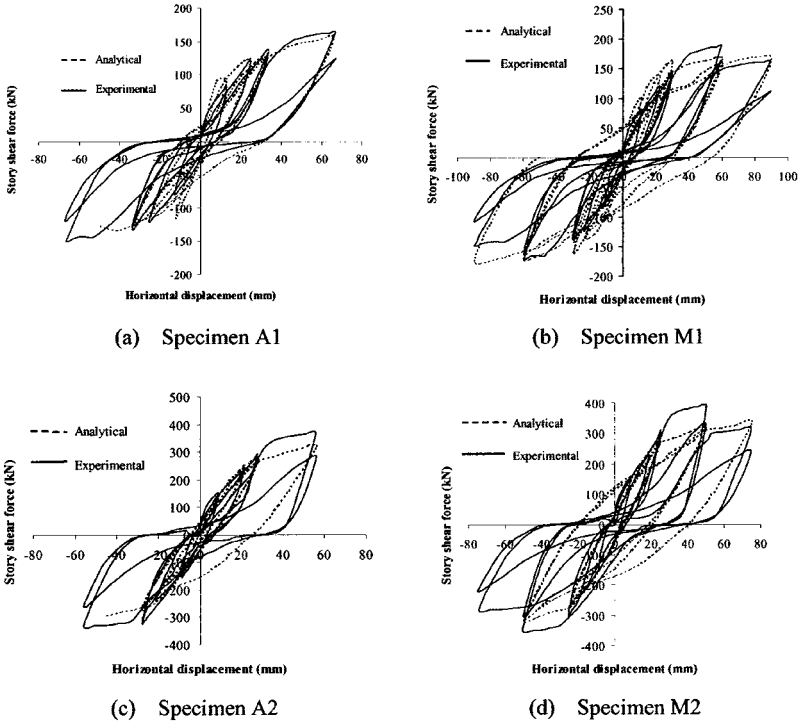

Fig. 1—Predicted story shear force versus horizontal displacement.

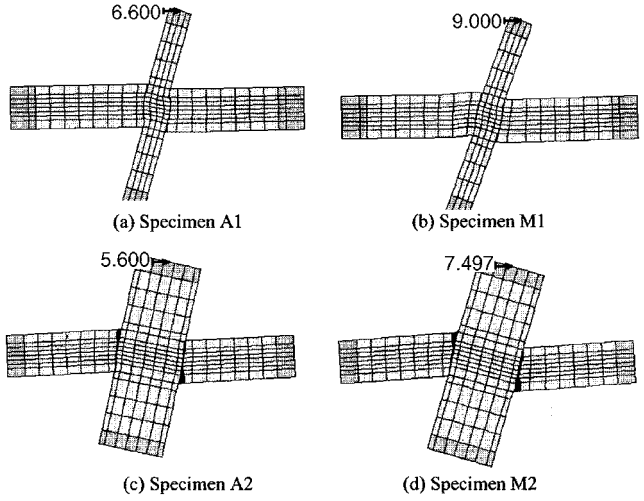

Fig. 2—Finite element meshes and deflection shapes of specimens of specimens using FEM software package.

actual positions of the reinforcement. In the FEM software package,[3] a nine-node quadrangular element is assumed for concrete under an in-plane stress condition; concrete plate element models have been constructed by combining the constitutive law for concrete and that for reinforcing bars. The constitutive law adopted for the cracked concrete is composed of the tension-stiffening model, the compression-stiffening model, and the shear transfer model. The elements at the ends of the beams and columns were set as elastic plates, and the rest of the elements were set as reinforced concrete plates. The anchorage of the beam longitudinal bars and column main bars was defined by using reinforced concrete joint plates, which were located at the boundaries of the joint core. During the test, bond deterioration along the beam longitudinal bars and column main bars was found; and for nonseismically detailed beam-column joints, the slippage of the steel bars was expected to occur. To simulate such conditions, in this study, the formulated bond-slip-strain relationship[6] mentioned previously was used. Nodes at both beam ends were restrained to displace in a vertical direction and be free in a horizontal direction. Lateral incremental displacement was applied at the column end of the specimen under a zero axial load. The load and displacement control loading history used in the experiment was also used in the analysis.

Computed responses of Specimens A1 and M1—The predicted and observed lateral load-displacement responses for Specimens A1 and M1 are shown in Fig. 1(a) and (b). From these two figures, it can be seen that the developed analytical model seems to accurately predict the experimentally observed response of the beam-wide column joints with or without joint shear reinforcement in terms of strength, ductility, and energy dissipation. It was found from the finite element analysis results that Specimen M1 achieved the horizontal displacement ductility factor of 3. Specimen A1 is only capable of reaching achieved the horizontal displacement ductility factors of approximately 2. Obvious pinching can be observed in the loop of the numerical results of Specimen A1, and the whole loops were very thin. These characteristics are similar to those observed in the experimental results. Figure 2(a) shows the global deformation of Specimen A1 at the stage of ductility factor 2. The deformation of the joint core is quite large. The story shear forces of Specimen A1 at each peak horizontal displacement are shown in Fig. 3(a). For Specimen M1, pinching can be observed in the analytical loops, but not very obviously when compared with the experimental loops. The specimen deformation at the stage of ductility factor 3 is found in Fig. 2(b). Extensive joint core deformation can also be observed. Figure 4(a) and (b) show the cracking patterns of Specimens A1 and M1 at the stage of ductility factors 2 and 3, respectively. Extensive cracking within the joint core region can be found in the early stages, and the cracks open widely as the horizontal displacement increases. At the end of the analysis, severe

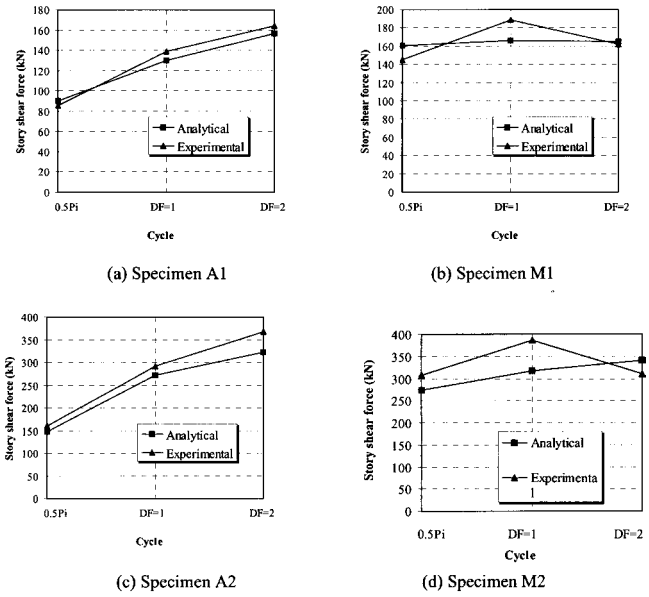

Fig. 3—Predicted story shear force of specimens.

cracking is found in the joint core. Figure 5(a) and (b) show the stress distributions in Specimens A1 and M1 at the stage of ductility factors 2 and 3, respectively. A diagonal compression stress zone can be found within the joint core, and a diagonal tension stress zone passed across it.

Computed responses of Specimens A2 and M2—The lateral load-displacement responses from the finite element analysis compare well with those of the tested subassemblies. From Fig. 1(c) and (d), the finite element analysis results show that Specimen M2 achieved the horizontal displacement ductility factor of 3 or 75 mm. Specimen A2, however, is only capable of reaching the horizontal displacement ductility factors of approximately 2. Obvious pinching cannot be observed in the loop of the numerical results of Specimen A2. Figure 2(c) and (d) present the global deformation of both Specimens A2 and M2 at the final failure stage. Extensive deformations occurred in the beam ends and the joint core region. The story shear forces of Specimens A2 and M2 at each peak horizontal displacement are shown in Fig. 3(c) and (d), respectively. The global deformations of Specimens A2 and M2 at the final failure stage are found in Fig. 2(c) and (d), respectively. Extensive joint core deformation can also be observed. Figure 4(c) and (d) show the cracking patterns of Specimens A2 and M2 at the stage of ductility factors 2 and 3, respectively. Extensive cracking within the joint core region and column faces is found in the early stage, and the cracks open widely as the horizontal displacement increases. When the ductility factor of 2 is reached, severe cracking was found in the joint core, and large cracks were formed at the column faces. Figure 5(c) and (d) show the stress distributions in Specimens A2 and M2 at the final stage of ductility factor.

Discussion of analysis results

Global behaviors of joints—The analysis results have shown that for all the specimens, the analytical lateral load-displacement hysteresis loops obtained from the finite element analysis are quite similar to those obtained from the experimental work. The predictions for the failure modes and the ultimate ductility capacities correlate well with the experimental results. This trend lends support to the use of the computational modeling techniques.

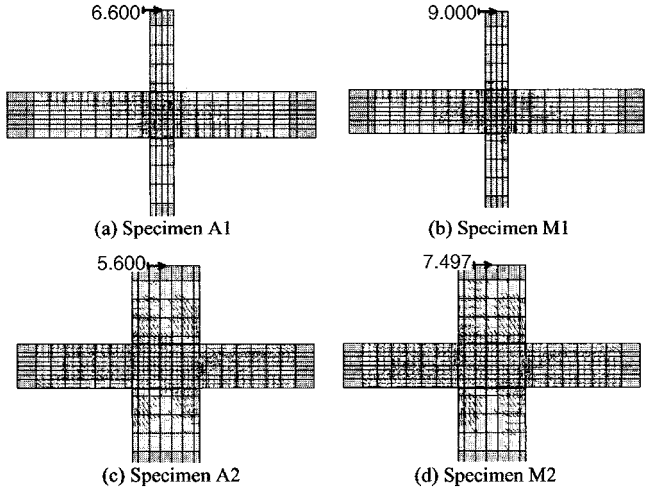

Fig. 4—Predicted cracking patterns of specimens.

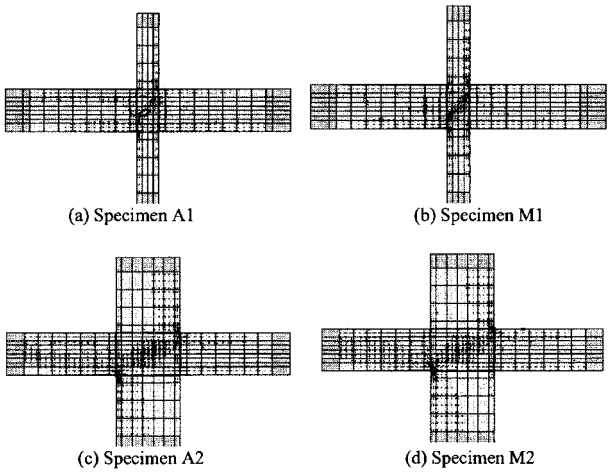

Fig. 5—Predicted compression and tension stresses in specimens.

Deformations, cracking patterns, and story shear forces—The finite element analysis results have demonstrated that deformations and cracking patterns obtained from the analysis results are very similar to those in the experimental work. In addition, story shear forces obtained from the analyses are similar to those of the experiments. This indicates that, based on well-established models, the finite element analysis is able to produce fairly accurate predictions of joint performances.

PARAMETRIC STUDY OF REINFORCED CONCRETE BEAM-WIDE COLUMN JOINTS

After calibration against the experimental results, a parametric study using the validated finite element models was performed to improve the understanding of the structural response of the beam-wide column joints on the effects of some critical parameters, such as joint transverse reinforcement, column axial loading, and beam bar diameters. The configurations and specifications of all other joints considered in the parametric investigation were the same as those presented in the previous paper.

Influence of joint transverse reinforcement on behavior of beam-wide column joints

As shown in the previous experimental study and the finite element analysis, specimens with joint transverse reinforcement

perform better than those specimens without joint transverse reinforcement. To explain such improvement, oblong and wall-like column joints with different joint transverse reinforcement ratios were further studied. The joint transverse reinforcement ratio ranges from 0 to 40% of the amount required by New Zealand Standard 3101.[11]

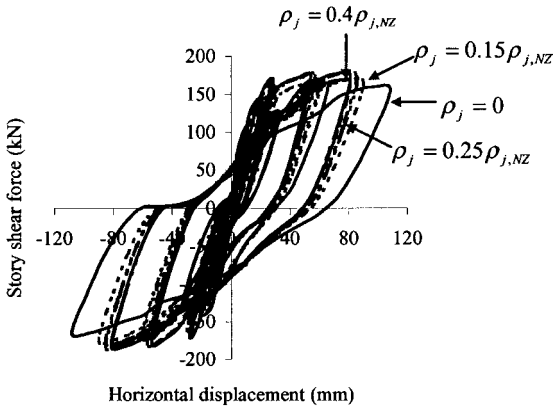

Fig. 6—Comparison of overall behavior among oblong joints with different joint transverse reinforcement ratio.

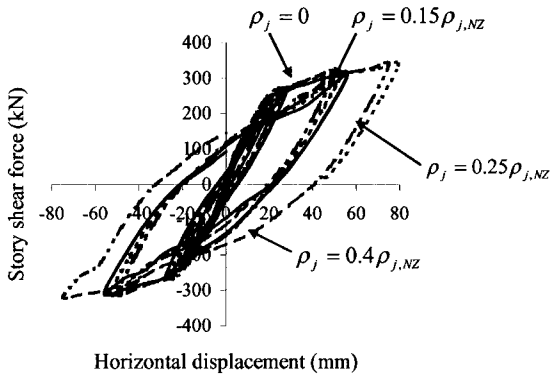

Fig. 7—Comparison of overall behavior among wall-like joints with different joint transverse reinforcement ratio.

Figure 6 and 7 show the overall behavior of the oblong joints and the wall-like column joints. It was observed that for both kinds of joints, the better the performance is, the more transverse reinforcement is contained in the joint core. The stiffness and the overall ductility increase as the ratio of joint transverse reinforcement increases. The explanation for such an improvement may be obtained by analyzing and comparing the principal compression stresses of the joints. Thus, in this parametric study, the maximum principal compression stresses occur in the regions close to the column and beam compression zones, such as Zones 1 and 4 in oblong joints (Fig. 8), or Zones 1 and 7 in wall-like column joints (Fig. 9). Experimental work, however, has nearly always shown that joint failure occurs through the crushing of the concrete at the joint center.[12] Therefore, a comparison of the principal compression stresses should be carried out on the joint central zones, and this would show more clearly the influence of joint transverse reinforcement.

Figure 8 shows the comparison of maximum principal compression stresses of oblong joints, observed in the central joint zones at different stages among four specimens, and in which joint transverse reinforcement ranged from 0, 15, and 25 to 40% of the amount required by NZS 3101.[11] It can be seen that for oblong joints, the maximum principal compression stresses observed in specimen, which contains less joint transverse reinforcement, are higher than those containing more, not only at every ductility level, but also at the final failure stage. Similar phenomenon can also be seen in Fig. 9, where the same comparison is made between wall-like column joints. At the same ductility level, the maximum principal compression stresses, observed in joints containing less transverse reinforcement, are higher than those containing more.

From the aforementioned comparison, it can be seen that at the same ductility level, a lower stress state is generated

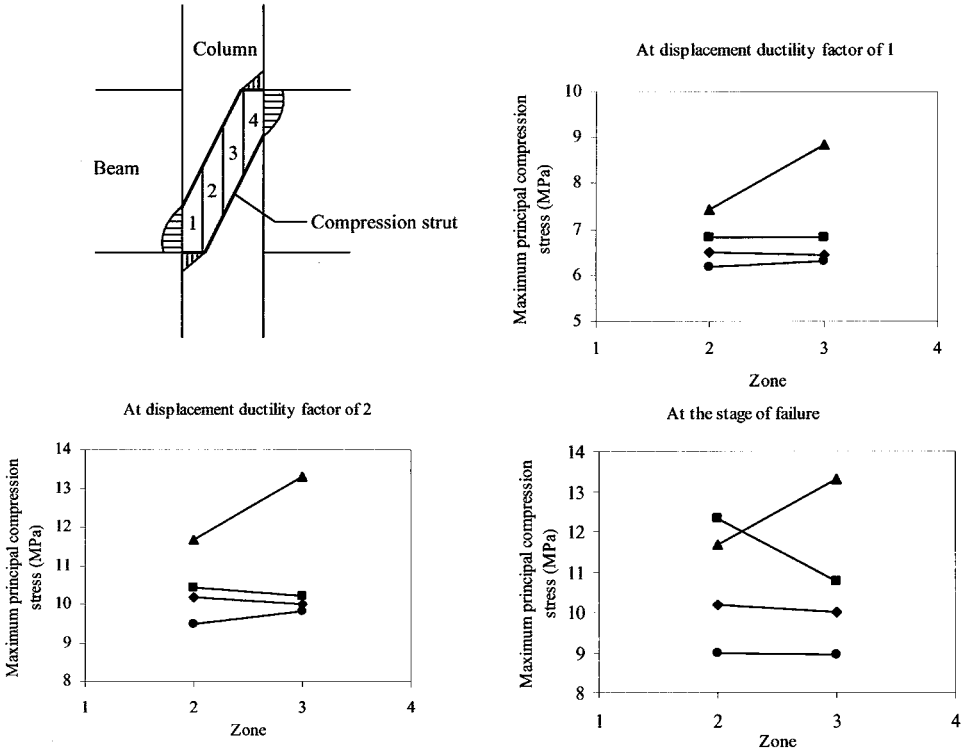

Fig. 8—Comparison of maximum principal compression stresses between oblong joints.

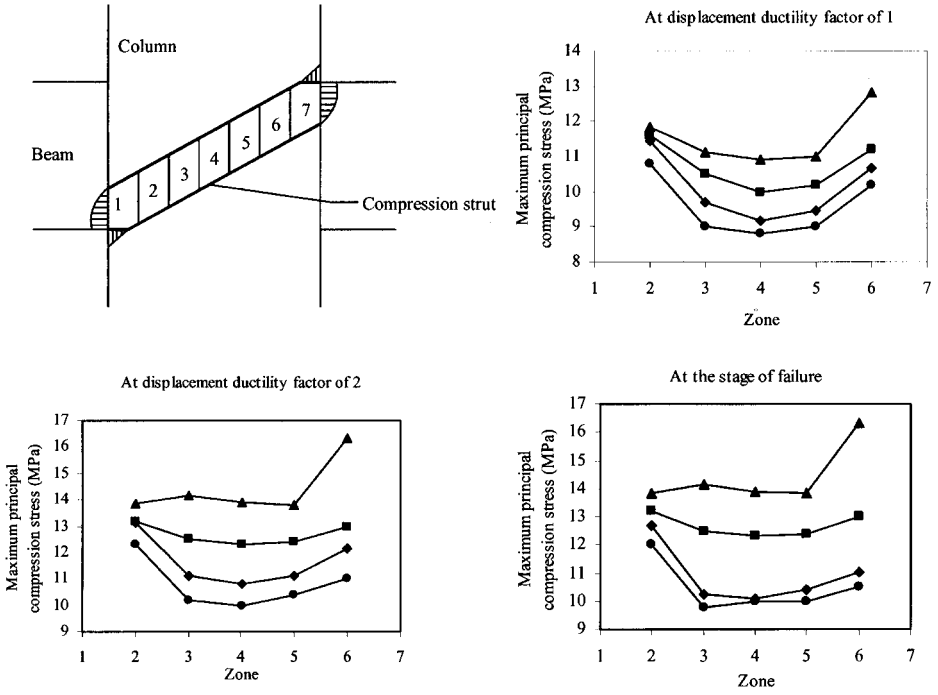

Fig. 9—Comparison of maximum principal compression stresses between wall-like column joints.

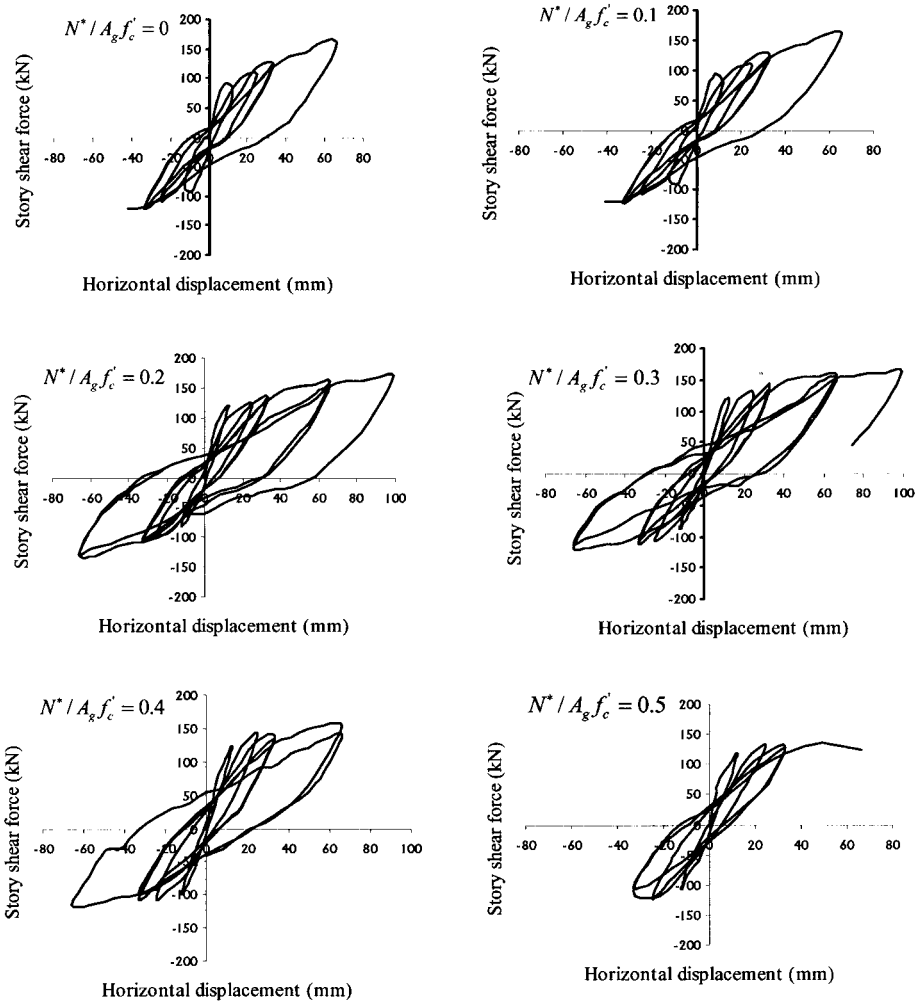

Fig. 10—Comparison of global behavior of oblong Joint A1 under different axial loading levels.

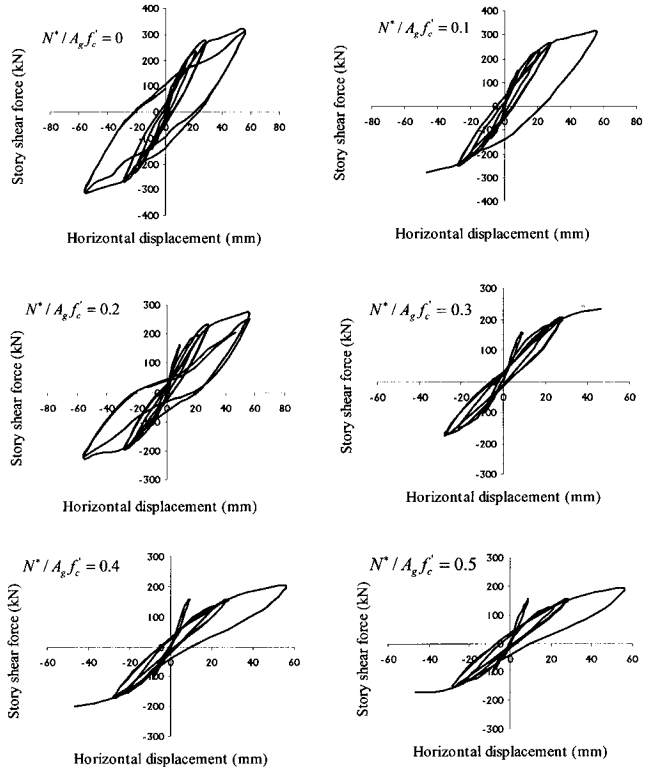

Fig. 11—Comparison of global behavior of wall-like column Joint A2 under different axial loading levels.

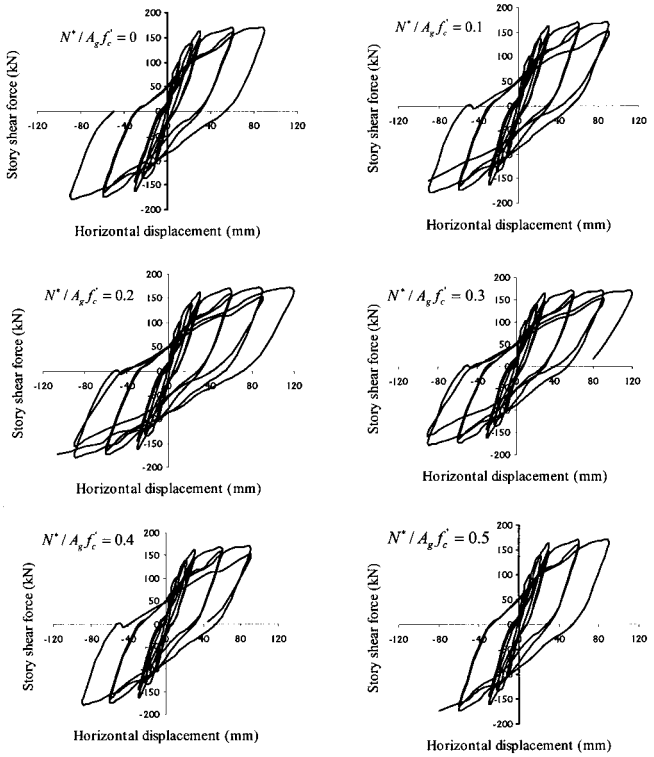

Fig. 12—Comparison of global behavior of oblong Joint M1 under different axial loading levels.

within specimens containing more transverse reinforcement when compared with specimens containing less. The joints without transverse reinforcement are easily overloaded, and as a result, they failed at an earlier ductility level stage. The aforementioned observations indicate that for joints sustaining reversed increasing cyclic deformations, the use of joint transverse reinforcement could improve the joints' behavior by reducing the principal compression stress level to a state lower than the concrete diagonal compression strength, which decreases with the increase of tension strains in a transverse direction. Adding the joint transverse reinforcement, however, cannot prevent the eventual joint failure. This is due to the progressive increase in the tensile strains in the transverse direction, which has been shown to severely reduce the diagonal compressive strength of the concrete;[13] thus, the yielding of the joint transverse reinforcement may fail to reduce the principal compression stress level further.

Influence of axial loads on behavior of beam-wide column joints

Hakuto, Park, and Tanaka[14] have already established a model to predict the seismic behavior of nonductile beam-column joints; however, this model did not take the axial loads into accounts. This limit prevents the application of this model from practical uses. Actually, axial loading is a critical parameter in the studies of beam-column joints, but the effect of axial loads on the seismic behavior of beam-column joints is still debated among researchers in this field. Paulay[15] pointed out that column axial force is beneficial to the joint shear resistance. Because the neutral axis depth in the column increases with axial compression, a larger portion of the bond forces from the beam bars can be assumed to be transferred to the diagonal strut. Thus, the contribution of the concrete to joint shear resistance will increase. This point of view was accepted by NZS 3101,[11] in which the concrete shear strength is considered to increase with the column axial loading. By comparing the experimental results in the late 1980s, however, Kurose et al.[16] pointed out that the level of axial force did not seem to influence joint shear strength any more. In a study conducted by Pessiki et al.,[17] two nonductile interior beam-column joints with different axial loading levels were tested. The test results, however, cannot be used to evaluate the influence of axial loading because both of the specimens failed due to the pullout of the embedded beam bottom bars instead of joint shear failure. Recently, a number of researchers[18,19] noticed that the effect of axial loads may vary at different axial loading levels or at different joint shear levels. By testing 10 interior beam-column joints, Fu et al.[19] pointed out that if the shear is high, the increase of axial loads is unfavorable, whereas if the shear is small, the increase of axial loading is favorable to the joints. In Lin's study,[18] it was found that axial compression in excess of $N^*/f_c'A_g \geq 0.3$ became detrimental to the joints.

To investigate the influence of axial loading on the seismic behavior of beam-wide column joints, in this attempt, the seismic behaviors of oblong Joints A1 and M1, and wall-like column Joints A2 and M2 under different axial loading levels were analyzed by the FEM software package. The same loading histories as those used in the analysis of specimens without axial loading were applied, and the corresponding story shear force versus horizontal displacement loops under different axial loading levels were listed (Fig. 10 to 13). Under the same reversed increasing cyclic loading history, the ultimate number of cycles a specimen can attain may be used as an index to compare the joint's behavior. The more cycles attained, the better it performs.

Figure 14 plots the comparison. It can be seen that for the oblong Joints A1 and M1, when the axial load increased from 0 to $0.2f_c'A_g$, the number of cycles increased correspondingly. When the axial load continued to increase, the number of cycles

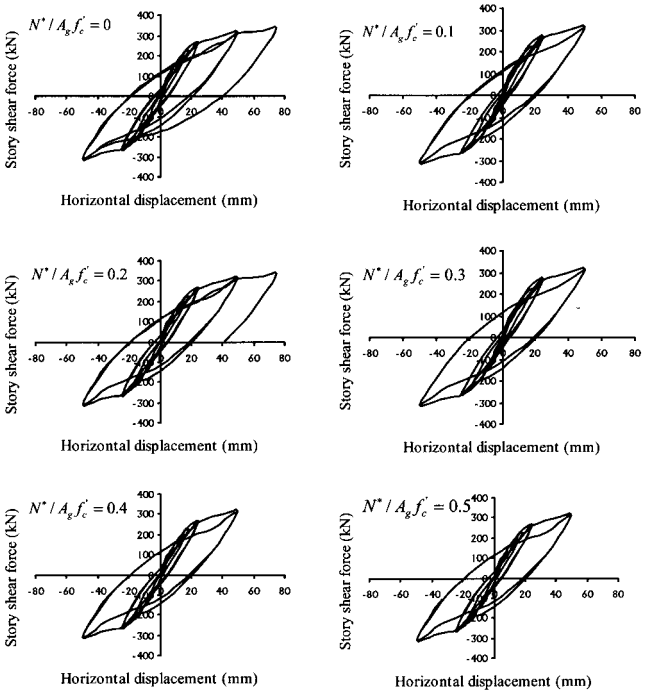

Fig. 13—Comparison of global behavior of wall-like column Joint M2 under different axial loading levels.

began to drop, and finally when the axial load attained $0.5f_c'A_g$, the number of cycles became less than the number when no axial load was applied. This may suggest that the axial load may be beneficial to the joint's behavior when it is less than $0.4f_c'A_g$; after that, the axial load may become detrimental. Similar conclusions were also drawn by Lin[18] that between $N^*/A_g f_c' = 0.1$ and 0.3, the axial compression load is beneficial to the joint, while when $N^*/A_g f_c' \geq 0.3$, the axial compression load becomes detrimental to the joint.

Different results, however, were found in the analysis of wall-like column Joints A2 and M2. As illustrated in Fig. 14, the best performances of the specimens were observed when the axial load attained zero and $0.2f_c'A_g$. At other axial loading levels, the performances were poor, especially when the axial load attained $0.3f_c'A_g$. Unlike Specimens A1 and M1, the axial load did not show any beneficial effect on the joint's behavior because when the axial load ranged from 0 to 0.5 $f_c'A_g$, the increase of the cycle number was not observed at any axial loading level.

Influence of larger-diameter longitudinal bars on bond deterioration

At interior beam-column joints, extremely high bond stresses can be developed when a reinforced concrete frame sustains large inelastic deformations due to seismic motions. Beam bars may be forced to yield in tension at one column face and be subjected to a large compressive stress at the opposite column face. Also, yield penetration along a beam bar from either face of an interior column may considerably reduce the effective anchorage length of the bar and increase deformations.

Thus, the limit for the ratio of bar diameters to the column depth is intended to ensure that a beam bar will not slip prematurely through the joint core during cyclic reversed inelastic displacements.[20,21] Currently in the New Zealand practice, it is regulated that[11]

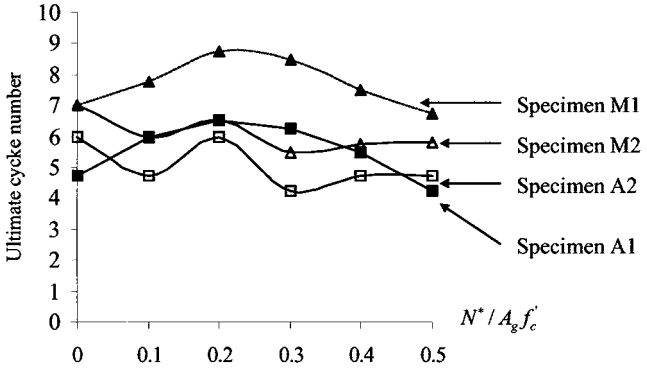

Fig. 14—Ultimate cycle number.

Table 1—Beam bar diameters used in oblong joints

Oblong joints				
d_b, mm	h_c, mm	d_b/h_c	d_b/h_c regulated by NZS3101:1995	d_b/h_c regulated by ACI-ASCE Committee 352
10	300	0.033	0.029	0.05
12	300	0.040	0.029	0.05
16	300	0.053	0.029	0.05

Table 2—Beam bar diameters used in wall-like column joints

Wall-like column joints				
d_b, mm	h_c, mm	d_b/h_c	d_b/h_c regulated by NZS3101:1995	d_b/h_c regulated by ACI-ASCE Committee 352
25	900	0.027	0.032	0.05
28	900	0.031	0.032	0.05
32	900	0.035	0.032	0.05

$$\frac{d_b}{h_c} \leq 3.3\alpha_f \frac{\sqrt{f'_c}}{a_o f_y} \quad (6)$$

where d_b is the diameter of the beam bars; h_c is the column height; $\alpha_f = 1.0$; $a_o = 1.25$; f_c' is the concrete compressive strength; and f_y is the steel tensile strength. In the American practice, however, a less strict regulation is applied[22]

$$\frac{d_b}{h_c} \leq 0.05 \quad (7)$$

The use of a wall-like column section could lead to some relaxation of the bond requirements in beam-column joints that are currently specified in a simplistic manner by the number of bar diameters of anchorage. This relaxation should be possible because bond-slippage passing through an interior beam-column joint depends on the column size. The deeper the column sections, the less the beam bar slip in the joints. On the other hand, the use of oblong column sections will lead to serious problems in design. Beam bar slip and pullout displacement increase and, hence, pinching of the hysteresis loops is noticeable.

In this study, to investigate the effect of the parameter d_b/h_c on joint behaviors, different beam bar diameters were used as listed in Table 1 and 2. The same loading histories like those used in the experiments of specimens were applied, and the corresponding story shear force versus horizontal

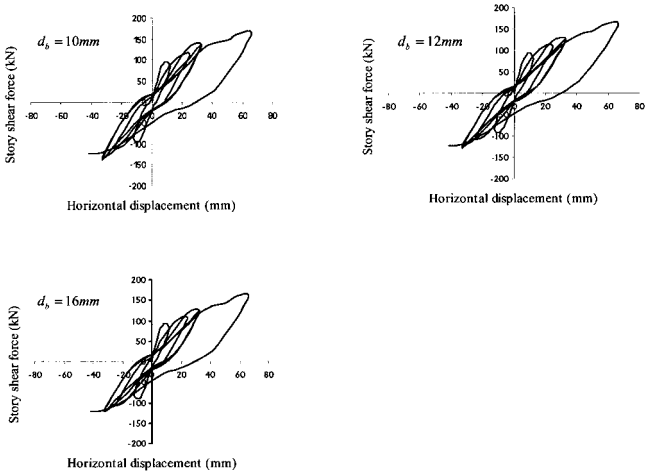

Fig. 15—Comparison of global behavior of oblong Joint A1 with different beam bar diameters.

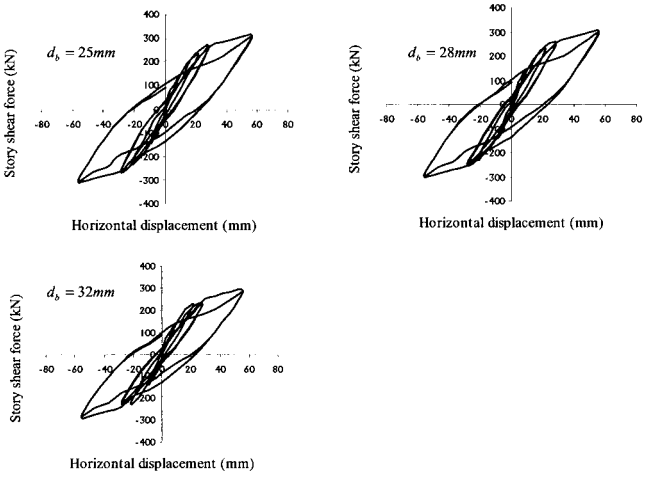

Fig. 16—Comparison of global behavior of wall-like column Joint A2 with different beam bar diameters.

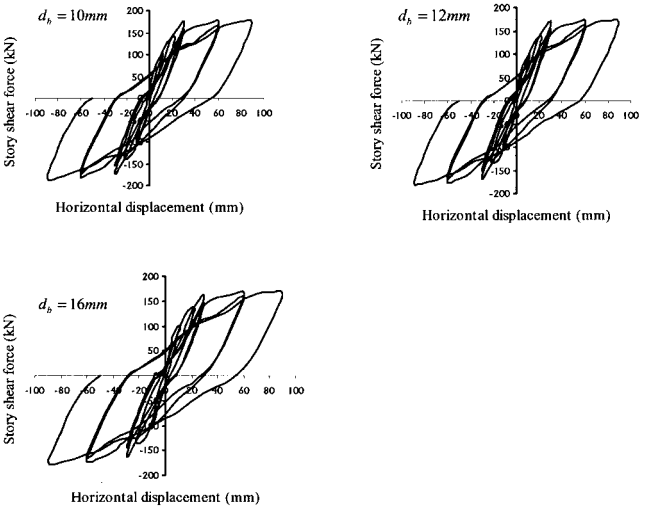

Fig. 17—Comparison of global behavior of oblong Joint M1 with different beam bar diameters.

displacement loops with different d_b/h_c ratios were listed (Fig. 15 to 18).

It was observed that for oblong Joints A1 and M1, by using the small-diameter beam bars, the peak strengths and the stiffness of the specimens were slightly increased. This is due mainly to the use of small-diameter beam bars, which caused less severe bond deterioration to occur. The global behaviors of the specimens did not change much, however, and the final failure patterns also did not change. For wall-like column Joints A2 and M2, no obvious influence was observed after using big diameter beam bars. This may be due mainly to the large column depth, which keeps the d_b/h_c ratio small enough to prevent the occurrence of bond deterioration. In addition, it was observed that for the oblong Joint M1, although joint transverse reinforcement was added, bond deterioration was still observed. This may suggest that using joint transverse reinforcement does not improve the bond condition.

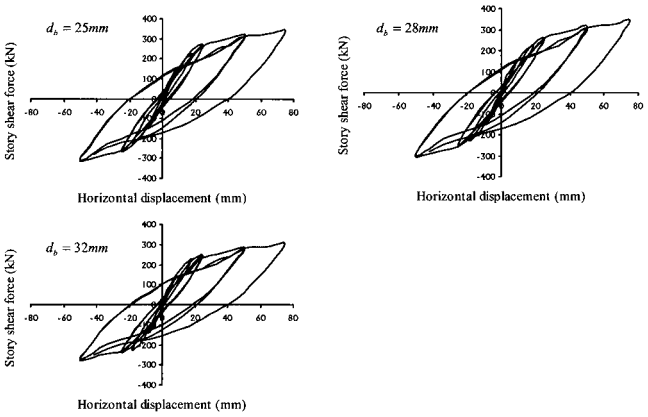

Fig. 18—Comparison of global behavior of wall-like column Joint M2 with different beam bar diameters.

CONCLUSIONS

To study the effect of several design parameters on seismic behavior of beam-wide column joints, numerical models are developed in this paper. The numerical model employs the finite element method. The FEM software is used for this purpose. Comparisons with the experimental results indicated that the finite element models used in this study were suitable and the corresponding analysis results were reliable. The agreement between the prediction and the experimental observation was judged good. Based on the results of this study, the following conclusions are drawn.

1. For beam-wide column joints, joint transverse reinforcement helped to maintain the strength of the specimen more than it helped to reduce the loss of stiffness. The modification of the reinforcing details had no obvious effect on improving the bond conditions because the bond conditions depend mainly on the ratio of beam and column main bar diameters to the depths of those columns and beams;

2. For an oblong joint, when $N^*/A_g f_c' < 0.4$, the axial compression load is beneficial to the joint, while when $N^*/A_g f_c' > 0.4$, the axial compression load becomes detrimental to the joint;

3. For a deep wall-like column joint, the finite element analysis results show that the joint's performance was better when the axial compression load was zero or $0.2 f_c' A_g$. Unlike the oblong joint, the effect of axial compression loading was not constant for the behavior of the wall-like column joint. It changed at various axial loading levels;

4. The d_b/h_c ratio influences the behavior of oblong joints more than that of the wall-like column joints. It is recommended that small-diameter beam bars be used in the oblong joints. It is also concluded that joint transverse reinforcement has no effect on the beam bar bond conditions. Using the joint transverse reinforcement does not improve the bond behavior; and

5. Current ACI-ASCE Committee 352 and NZS 3101 design provisions seem overly conservative in the use of small-diameter beam bars in the wall-like column joints. Due to the large dimension of the depth of wall-like column joints, the influence of the d_b/h_c ratio to the global behavior of these joints has been eliminated to a negligible value. Thus, it is recommended that no diameter restriction be set on the use of beam bars in wall-like column joints.

ACKNOWLEDGMENTS

The financial assistance provided by the Protective Technology Research Center in the School of Civil and Structural Engineering at Nanyang Technological University, Singapore, is gratefully acknowledged.

NOTATIONS

A_g	=	gross area of column
b_j	=	effective joint width
c	=	constant = 3
D	=	diameter of bar
d_b	=	diameter of reinforcing bar
f_c'	=	concrete compressive strength
h_c	=	column depth
k	=	constant = 0.73
N^*	=	axial compression load
P_i	=	horizontal load at top of column associated with theoretical flexure strength
S	=	slip
s	=	nondimensional slip, = $1000S/D$
V_{jh}	=	joint shear force
v_{jh}	=	joint nominal shear stress
ρ_j	=	ratio of joint transverse reinforcement
$\rho_{j,NZ}$	=	ratio of joint transverse reinforcement required by NZS 3101:1995

REFERENCES

1. BS 8110, "Structural Use of Concrete, Part 1. Code of Practice for Design and Construction," British Standard, 1997, 122 pp.

2. Pan, T.-C.; Megawati, K.; and Lee, C. L., "Seismic Hazard Assessment of Singapore—Effects of Long Distance Major Earthquakes," *Proceedings of the International Conference on Advances in Structural Dynamics*, V. I, Hong Kong, Dec. 13-15, 2000, pp. 233-240.

3. UC-win/WCOMD, "Beginners Guide to UC-win/WCOMD," University of Tokyo, 1997.

4. Maekawa, K., and Okamura, H., "The Deformational Behavior and Constitutive Equation of Concrete Using Elasto-Plastic and Fracture Model," *Journal of Faculty of Engineering*, University of Tokyo(B), V. 37, No. 2, 1983, pp. 253-328.

5. Aoyagi, Y., and Yamada, K., "Strength and Deformation Characteristics of Reinforced Concrete Shell Elements Subjected to In-Plane Forces," *Proceedings of Japanese Society of Civil Engineers*, No. 331, 1983, pp. 167-180.

6. Hajime, O., and Kohichi, M., *Nonlinear Analysis and Constitutive Models of Reinforced Concrete*, 1991, 182 pp.

7. Okamura, H.; Maekawa, K.; and Sivasubra, S., "Verification of Modeling for Reinforced Concrete Finite Element, Finite Element Analysis of Reinforced Concrete Structures," *Journal of Structural Engineering*, ASCE, 1985, pp. 528-543.

8. Collins, M. P., and Vecchio, F., "The Response of Reinforced Concrete to In-Plane Shear and Normal Stresses," University of Toronto, 1982.

9. Shima, H.; Chou, L.; and Okamura, H., "Micro and Macro Models for Bond Behavior in Reinforced Concrete," *Journal of Faculty of Engineering*, University of Tokyo(B), V. 39, No. 2, 1987, pp. 133-194.

10. Kato, B., "Mechanical Properties of Steel under Load Cycles Idealizing Seismic Action," *CEB Bulletin D'Information*, No. 131, 1979, pp. 7-27.

11. New Zealand Standard 3101, "Concrete Structures Standard (1995): Part 1—The Design of Concrete Structure," 1995, 256 pp.

12. Paulay, T., and Priestley, M. J. N., *Seismic Design of Reinforced Concrete and Masonry Buildings*, John Wiley & Sons, New York, 1992, 744 pp.

13. Vecchio, V. J., and Collins, M. P., "The Modified Compression-Filed Theory for Reinforced Concrete Elements Subjected to Shear," ACI JOURNAL, *Proceedings* V. 83, No. 2, Mar.-Apr. 1986, pp. 219-231.

14. Hakuto, S.; Park, R.; and Tanaka, H., "Retrofitting of Reinforced Concrete Moment Resisting Frames," *Research Report* 95-4, Department of Civil Engineering, University of Canterbury, Christchurch, New Zealand, 1995, 390 pp.

15. Paulay, T., "Equilibrium Criteria for Reinforced Concrete Beam-Column Joints," *ACI Structural Journal*, V. 86, No. 6, Nov.-Dec. 1989, pp. 635-643.

16. Kurose, Y.; Guimaraes, G. N.; Liu, Z.; Kreger, M. E.; and Jirsa, J. O., "Study of Reinforced Concrete Beam-Column Joints under Uniaxial and Biaxial Loading," *PMFSEL Report* No. 88-2, Department of Civil Engineering, University of Texas at Austin, Dec. 1988, 146 pp.

17. Pessiki, S. P.; Conley, C. H.; Gergely, P.; and White, R. N., "Seismic Behavior of Lightly Reinforced Concrete Column and Beam-Column Joint Details," *NCEER Technical Report* No. 90-0014, State University of New York at Buffalo, 1988.

18. Lin, C. M., "Seismic Behavior and Design of Reinforced Concrete Interior Beam-Column Joints," *Research Report* 2000-1, Department of Civil Engineering, University of Canterbury, Christchurch, New Zealand, 2000, 471 pp.

19. Fu, J.; Chen, T.; Wang, Z.; and Bai, S., "Effect of Axial Load Ratio on Seismic Behavior of Interior Beam-Column Joints," *Paper* No. 2707, 12th World Conference on Earthquake Engineering, 2000.

20. Blakeley, R. W. G.; Megget, L. M.; and Priestley, M. J. N., "Seismic Performance of Two Full-Size Reinforced Concrete Beam-Column Joint Units," *Bulletin of the New Zealand National Society for Earthquake Engineering*, V. 8, No. 1, Mar. 1975, pp. 38-69.

21. Blakeley, R. W. G.; Edmonds, F. D.; Megget, L. M.; and Wood, J. H., "Cyclic Load Testing of Two Reinforced Concrete Joints," *Bulletin of the New Zealand National Society for Earthquake Engineering*, V. 12, No. 3, Sept. 1979, pp. 238-255.

22. Joint ACI-ASCE Committee 352, "Recommendations for Design of Beam-Column Joints in Monolithic Reinforced Concrete Structures (ACI 352R-91)," American Concrete Institute, Farmington Hills, Mich., June 1991, 21 pp.